# Synthesis, Crystal Structure, and Second-Order Nonlinear Optical Properties of a New Phase-Matchable Cyanine Dye

Pascal G. Lacroix* and Isabelle Malfant

*Laboratoire de Chimie de Coordination, 205 route de Narbonne, 31077 Toulouse Cedex, France*

Corinne Payrastre and Jean-Gérard Wolf*

*Laboratoire de Synthèse et Physicochimie Organique, UPRESA 5068, Université Paul Sabatier, 31062 Toulouse Cedex, France*

Jacques Bonvoisin

*Centre d'Elaboration des Matériaux et d'Etudes Structurales, 29 rue J. Marvig, 31055 Toulouse Cedex, France*

Keitaro Nakatani

*P.P.S.M., CNRS URA 1906, Ecole Normale Supérieure de Cachan, Avenue du Président Wilson, 94235 Cachan Cedex, France*

*Received November 11, 1997. Revised Manuscript Received February 13, 1998*

A new chiral hemicarboxonium salt, (ephem)($BF_4$), was synthesized by action of α-1-((methylamino)ethyl)benzyl alcohol, (−)-ephedrine, on a carboxonium tetrafluoroborate salt. The compound crystallizes in monoclinic space group $P2_1$. $a = 11.153(1)$ Å, $b = 8.187(1)$ Å, $c = 16.104(1)$ Å, $\beta = 91.26(1)°$, $Z = 2$. The molecular origin of the nonlinearity was calculated using the INDO/SCI-SOS approach. The static molecular hyperpolarizability ($\beta_0$) is equal to $10.7 \times 10^{-30}$ $cm^5$ $esu^{-1}$. The compound is phase matchable and exhibits an efficiency around 20 times that of urea at 1.097 $\mu$m. The orbital description of the electronic transitions reveals that the carbon skeleton is mainly responsible for the NLO response. The possibility of growing large single crystals (>0.5 $mm^3$) associated with a good transparency ($\lambda_{max} = 420$ nm) suggests that pentamethinium salts may be an interesting family of materials for second-order optical nonlinearities.

## Introduction

Over the last two decades, intense activity in the field of organic synthesis has demonstrated the relevance of organic media for second-order nonlinear optical (NLO) properties.[1] The basic strategy of using electron-donor and electron-acceptor substituents to polarize the $\pi$-electron system of organic materials, thereby creating the possibility of a second-order NLO response, has been recognized for many years. These efforts have first focused on relatively simple donor−acceptor organic systems with particular emphasis on the *p*-nitroaniline family.[2,3] More recently, highly polar cationic cyanine dyes have emerged as promising candidates for molecular engineering of chromophoromes in various acentric environements by virtue of the nature of the counteranion.[4,5] These compounds exhibit a NLO response that, in some cases, is several orders of magnitude higher than that of inorganic materials currently available, such as KDP or $LiNbO_3$.[6] Nevertheless, the main bottlenecks to the development of a second-order NLO material is the compulsory noncentrosymmetric environment of the chromophores if the molecular hyperpolarizability ($\beta$) is to contribute to an observable bulk nonlinear susceptibility ($\chi^{(2)}$).[6] Various strategies have been reported for the engineering of molecules into acentric arrangements by intercalation into layered materials[5] or using the promising poled polymer approach[7] but the most traditionnal approach which guarantees stable acentric organizations of NLO chromophores in the solid state is based on the possibility of growing large noncentrosymmetric single crystals

(1) Zyss, J. *Molecular Nonlinear Optics* Academic Press: New York, 1994.

(2) Zyss, J.; Chemla, D. S. Quadratic Nonlinear Optics and Optimization of the Second-Order Nonlinear response of Molecular Crystals. In *Nonlinear Optical Properties of Organic Molecules and Crystals*; Chemla, D. S., Zyss, J., Eds.; Academic Press: New York, 1987.

(3) Nicoud, J. F.; Twieg, R. J. Design and Synthesis of Organic Molecular Compounds for Efficient Second-Harmonic Generation. In *Nonlinear Optical Properties of Organic Molecules and Crystals*; Chemla, D. S., Zyss, J., Eds.; Academic Press: New York, 1987.

(4) (a) Marder, S. R.; Perry, J. W.; Yakymyshyn, C. P. *Chem. Mater.* **1994**, *6*, 1137. (b) Marder, S. R.; Perry, J. W.; Schaefer, W. P. *Science* **1989**, *245*, 626.

(5) Lacroix, P. G.; Clément R.; Nakatani, K.; Zyss, J.; Ledoux, I. *Science* **1994**, *263*, 658.

(6) Williams, D. J. *Angew. Chem., Int. Ed. Engl.* **1984**, *23*, 690

(7) Eich, M.; Bjorklund, G. C.; Yoon, D. Y. *Polym. Adv. Technol.* **1990**, *1*, 189.

S0897-4756(97)00734-5 CCC: $15.00 
Published on Web 04/03/1998

**Scheme 1**

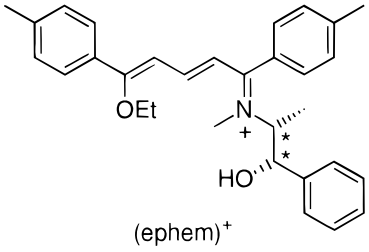


with a highly phase-matchable coefficient.[8] Therefore, the search toward new molecular materials has to be conducted in two directions to maximize both molecular ($\beta$) and bulk ($\chi^{(2)}$) nonlinearities.

Following this goal, this paper reports on the molecular and bulk second-order NLO properties of a new pentamethinium salt, belonging to a class of polymethine dyes used as spectral sensitizers in photography[9] and in photovoltaic[10] and xerographic[11] technology. The selected structure is shown in Scheme 1. It consists of a donor−acceptor substituted polymethinium cation, which ensures changes in dipole moments upon electronic transitions and hence the molecular second-order NLO response.

To overcome problems related to possible centrosymmetry of the crystal structure, we have synthezised a chiral derivative using an ephedrin substituted on the amine moieties. This (−)-ephedrin hemicarboxonium cation will be called ephem$^+$ for clarity. The NLO properties of (ephem)($BF_4$) will be discussed in relation with its crystal structure and its molecular hyperpolarizability.

## Experimental Section

**Starting Materials and Equipment.** The UV−visible spectrum was recorded on a Perkin-Elmer Lambda 9 spectrophotometer. Nuclear magnetic resonance spectra were obtained on a multinuclear Bruker AC 250 spectrometer operating in the Fourier transform mode at 250.13 ($^1$H) or 62.89 ($^{13}$C) MHz. The mass spectrum was obtained on a Nermag R 10 spectrometer with chemical ionization by $NH_3$. The infrared spectrum was obtained on a Perkin-Elmer 883 spectrometer from 200 to 4000 cm$^{-1}$. Elemental analysis was performed by the "service de microanalyse" (INP-ENSCT) in Toulouse, France.

**Synthesis of 1-Ethoxy-5-amino([1*R*,2*S*]-*N*-(2-hydroxy-1-methyl-2-phenyl)-*N*-methyl)-1,5-bis(*p*-methylphenyl)-pentadienylium Tetrafluoroborate ((ephem)($BF_4$)).** To a solution of 0.479 g (1.14 mmol) of 1,5-diethoxy-1,5-bis(*p*-methylphenyl)pentadienylium tetrafluoroborate (also called carboxonium salt)[12] in 10 mL of anhydrous acetonitrile, was added 0.187 g (1.14 mmol) of (−)-ephedrine in 20 mL of anhydrous $CH_3CN$. The mixture was stirred under an argon atmosphere for 4 h at room temperature. After evaporation of the solvent, the residual oil was washed several times with pentane and then crystallized in ethanol. Orange crystals, yield 72%, mp 209 °C: $^1$H NMR ($CDCl_3$) $\delta$ (ppm), $J$ (Hz) 1.30 (d, 3H, $J$ = 6.7, C$H_3$−CH); 1.40 (t, 3H, $J$ = 7.0, C$H_3$−$CH_2$); 2.31 and 2.37 (s, 3H, C$H_3$−$C_6H_4$); 3.69 (s, 3H, N−$CH_3$); 3.78 (d, 1H, $J$ = 5.6, OH); 4.03 (qd,1H, $J$ = 4.9, $J$ = 6.7, $CH_3$−C$H$); 4.19 (q, 2H, $CH_3$−C$H_2$); 5.07 (t, 1H, $J$ = 5.0 C$H$−OH); 6.26 (X part of ABX system, $J_{BX}$ = 11.5, $H_4$); 6.73 (B part of ABX syst, $J_{BX}$ = 11.5, $J_{BA}$ = 13.9, $H_3$), 6.83 (dd, 1H, $J$ = 6.2, $J$ = 1.5, $H_{arom}$), 6.87 (A part of ABX system., $J_{AB}$ = 13.9, $H_2$), 6.89−7.26 (m, 12H, $H_{arom}$); $^{13}$C NMR ($CDCl_3$) $\delta$ (ppm) 12.3 (*C*$H_3$−$CH_2$); 14.3 *C*$H_3$−CH); 21.3 and 21.4 (*C*$H_3$−$C_6H_4$); 36.4 (N−$CH_3$); 66.2 ($CH_3$−*C*H); 66.5 ($CH_3$−*C*$H_2$); 74.1 (CH−OH); 104.6 ($C_4$); 116.8 ($C_2$); 125.8−141.3 ($C_{arom}$); 162.6 ($C_3$); 175.0 ($C_5$); 176.5 ($C_1$); MS (DCI, $NH_3$) 454 M$^+$. Anal. Calcd for $C_{31}H_{36}NO_2BF_4$ (541.44): C 68.77, H 6.70, N 2.59. Found: C 68.58, H 6.71, N 2.52. IR (KBr) 1086 cm$^{-1}$ ($BF_4^-$), [a]$^{20}$ = +137° ($c$ = 0.053, $CH_3CN$, Hg lamp 578 nm), UV−vis ($CH_2Cl_2$) $\lambda_{max}$ = 420 nm, $\epsilon_{max}$ = 46 000 mol$^{-1}$ L cm$^{-1}$.

**Table 1. Structure Data Collection and Refinement for (ephem)($BF_4$)**

| | |
|---|---|
| formula | $C_{31}H_{36}BF_4NO_2$ |
| $M_w$ | 541.44 |
| crystal color | orange yellow |
| crystal dimensions (mm) | 0.8 × 0.3 × 0.1 |
| temp, K | 180 |
| crystal system | monoclinic |
| space group | $P2_1$ |
| $a$, Å | 11.153 |
| $b$, Å | 8.187 |
| $c$, Å | 16.104 |
| $\beta$, deg | 91.26 |
| $Z$ | 2 |
| $d$(calc), g cm$^{-1}$ | 1.22 |
| $F_{000}$ | 572.2 |
| $\mu$(Mo K$\alpha$), cm$^{-1}$ | 0.869 |
| diffractometer | IPds Stoe |
| radiation (Mo K$\alpha$), Å | 0.71069 |
| scan type | $\phi$ |
| 2$\theta$ range, deg | 2.9 < 2$\theta$ < 48.4 |
| no. of measured reflns | 11806 |
| no. of independent reflns | 4607 |
| intensities > 2$\sigma$($I$) | 3267 |
| no. of parameters | 361 |
| $R^a$ | 0.0677 |
| $R_w{}^b$ | 0.0693 |

[a] $R = \Sigma(||F_o| - |F_c||)/\Sigma(|F_o|)$. [b] $R_w = \Sigma w(|F_o| - |F_c|)^2/\Sigma w(F_o)^2]^{1/2}$.

**X-ray Data Collection and Structure Determination.** The data were collected at 180 K on a Stoe imaging plate diffraction system (IPDS) equipped with an Oxford Cryosystems cooler device. The crystal-to-detector distance was 80 mm. 167 exposures (3 min/exposure) were obtained with 0 < $\varphi$ < 250.5° and with the crystals rotated through 1.5° in $\varphi$. Owing to the rather low $\mu x$ value (0.869 cm$^{-1}$), no absorption correction was considered.

The structure was solved by direct methods (Shelxs-86)[13] and refined by least-squares procedures on $F_{obs}$. H(31) and H(41) were located on difference Fouriers maps, while the other hydrogen atoms were introduced in the calculation in idealized positions ($d$(CH) = 0.99 Å) and their atomic coordinates were recalculated after each cycle. They were given isotropic thermal parameters 20% higher than those of the carbon to which they are attached. The coordinates of the H(20) atom attached to the O(2) atom was not refined and was given a fixed isotropic thermal parameter of 0.05. Least-squares refinements were carried out by minimizing the function $\sum w(|F_o| - |F_c|)^2$, where $F_o$ and $F_c$ are the observed and calculated structure factors. The weighting scheme used in the last refinement cycles was $w = w'[1 - (\Delta F/6\sigma(F_o)^2]^2$, where $w' = 1/\sum_1^n A_r T_r(x)$ with four coefficients $A_r$ for the Chebyshev polynomial $A_r T_r(x)$, where $x$ was $F_c/F_c$(max).[14] Models reached convergence with $R = \Sigma(||F_o| - |F_c||)/\Sigma(|F_o|)$ and $Rw = \sum w(|F_o| - |F_c|)^2/\sum w(F_o)^2]^{1/2}$, having values listed in Table 1. Criteria for a satisfactory complete analysis were the ratios of rms shift

(8) Zyss, J.; Oudar, J. L. *Phys. Rev. A* **1982**, *26*, 2028.
(9) Daehne, S. *Photog. Sci. Eng.* **1979**, *23*, 219. James, T. H. *Adv. Photochem.* **1986**, *13*, 329.
(10) McEvoy, A. J.; Graetzel, M. *Sol. Energy Mater. Sol. Cells* **1994**, *32*, 221.
(11) Law, K. Y. *Chem. Rev.* **1993**, *93*, 449.
(12) Pikus, A. L.; Feigel'man, V. M.; Mezheritskii, V. V. *Zh. Org. Khim.* **1989**, *25*, 2603.
(13) Sheldrick, G. M. *SHELXS86, Program for Crystal Structure Solution*; University of Göttingen: Göttingen, Germany, 1986.
(14) Prince, E. *Mathematical Techniques in Crystallography*; Springer-Verlag: Berlin, 1982.

to standard deviation of less than 0.1 and no significant features in final difference maps. Details of data collection and refinement are given in Table 1.

The calculations were carried out with the CRYSTALS package programs[15] running on a PC. The drawing of the molecule was realized with the help of CAMERON.[16] Full interatomic distances and bond angles, fractional atomic coordinates, and the equivalent thermal parameters for all atoms and anisotropic thermal parameters for non-hydrogen atoms have been deposited at the Cambridge Crystallographic Data Center.

**SHG Measurements.** The measurements of second harmonic generation (SHG) intensity were carried out by the Kurtz−Perry powder technique,[17] using a picosecond Nd:YAG pulsed (10 Hz) laser operating at $\lambda = 1.064\ \mu$m. For measurements at 1.907 $\mu$m, the fundamental beam of a nanosecond Nd:YAG pulsed laser was focused in a hydrogen cell, and the Stokes-shifted radiation was used as an additional frequency. The SHG signal was selected through a suitable interference filter, detected by a photomultiplier, and recorded on an ultrafast Tektronic TDS620B oscilloscope. Samples were calibrated powders obtained by crystals grinding in the range 50−80, 80−120, and 120−180 $\mu$m.

**Calculation of NLO Response.** The all-valence INDO/S (intermediate neglect of differencial overlap) method[18] in connection with the sum-over-state (SOS) formalism[19] was employed. Details of the computationally efficient INDO-SOS-based method for describing second-order molecular optical nonlinearities have been reported elsewhere.[20] The calculation of electronic transitions was performed using the commercially available CAChe work system (Oxford Molecular). The monoexcited configuration interaction (MECI) approximation was employed to describe the excited states. The 81 energy transitions between the nine highest occupied molecular orbitals and the nine lowest unoccupied ones were chosen to undergo CI mixing. The calculation of molecular hyperpolarizabilities was performed using the commercially available MSI software package INSIGHT II (4.0.0). Although the nature and position of a counteranion have been reported to strongly influence the NLO response in some cases,[21] $BF_4^-$ was not introduced in the calculation. However, the agreement between experimental and calculated spectra suggests that the calculation is qualitatively reliable.

## Results and Discussion

**Synthesis and Crystal Growth.** A generalization of the method first reported by Mezheritskii[12] has been widely used in our group to obtain various dissymmetric pentamethinium salts.[22] For obvious safety reasons, $BF_4^-$ anion was preferred instead of $ClO_4^-$ reported in the original synthesis. Interestingly, large single crystals suitable for X-ray diffraction studies were easily grown by slow evaporation of a saturated solution in ethanol. Typical crystal sizes are 1.5 × 0.5 × 0.3 mm which is strongly indicative of good crystal growth abilities for (ephem)($BF_4$). This possibility is especially worthwhile when a situation of phase matching is observed in the material.

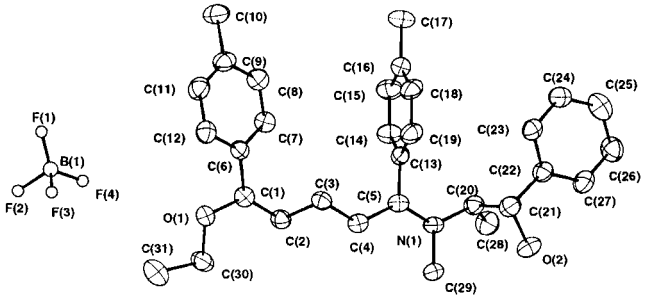


**Figure 1.** Atom labeling and thermal vibration ellipsoids for (ephem)($BF_4$). H atoms are omitted for clarity.

**Structure Description.** Figure 1 illustrates the (ephem)($BF_4$) molecule with the atomic numbering scheme employed. The structure consists of discrete ephem$^+$ cations and $BF_4^-$ anions, with no atoms in a special position. Two molecules are present is the crystal cell, which refer to one another by a helicoidal $2_1$ axis along *b*. Several attempts to treat the disorder in $BF_4^-$ anions were unsuccessful, even at 180 K. These species being expected to play no role in the nonlinearity, no further investigations were conducted on this disorder.

The main point of interest about the molecular structure concerns the true extent of the $\pi$-system involved in the intramolecular charge transfer and hence the NLO response. The C(1) to C(5) linkage, which is expected to play a major role in the charge transfer and the C(6) to C(12) methylphenyl group can be described as being roughly coplanar, with the largest deviation of 0.61 Å being observed at the C(7) atom. Therefore all carbon atoms located in this plane are expected to be involved in the frontier orbital description. Surprisingly, the angle between this mean plane and the second ring (C(13) to C(19)) is equal to 94.37°. From this observation, it can be expected that this latter ring will likely be very slightly involved in the optical transitions, which could enlarge the asymmetry of the electronic properties and hence the molecular NLO response.

**Molecular Origin of the Nonlinearity.** The optimization of materials for NLO devices first requires an in-depth understanding of the properties at the molecular scale. The widely used measurement (EFISH) for determinating $\beta$ is not applicable for measuring the second-order response of charged molecules. Theory, then, can play a crucial role for predicting the magnitude, sign, orientation, and origin of the NLO response. The theoretical $\beta$ (vectorial part of $\beta$) values are reported in Table 3 at different laser frequencies. The values are larger than that of paranitroaniline ($\beta = 11 \times 10^{-30}$ cm$^5$ esu$^{-1}$ at 1.907 $\mu$m),[23,24] although no strong donor, such as $-NH_2$ substituent, is present in the molecular structure. This rather surprising result encouraged us

(15) Watkin, D. J.; Prout, C. K.; Carruthers, J. R.; Betteridge, P. W. *CRYSTALS Issue 10*; Chemical Crystallography Laboratory, University of Oxford, Oxford, 1996.

(16) Watkin, D. J.; Prout, C. K.; Pearce, L. J. *CAMERON*; Chemical Crystallography Laboratory, University of Oxford, Oxford, 1996.

(17) (a) Kurtz, S. K.; Perry, T. T. *J. Appl. Phys.* **1968**, *39*, 3798. (b) Dougherty, J. P.; Kurtz, S. K. *J. Appl. Crystallogr.* **1976**, *9*, 145.

(18) (a) Zerner, M.; Loew, G.; Kirchner, R.; Mueller-Westerhoff, U. *J. Am. Chem. Soc.* **1980**, *102*, 589. (b) Anderson, W. P.; Edwards, D; Zerner, M. C. *Inorg. Chem.* **1986**, *25*, 2728.

(19) Ward, J. F. *Rev. Mod. Phys.* **1965**, *37*, 1.

(20) Kanis, D. R.; Ratner, M. A.; Marks, T. J. *Chem. Rev.* **1994**, *94*, 195.

(21) Di Bella, S.; Fragalà, I.; Ratner, M. A.; Marks, T. J. *Chem. Mater.* **1995**, *7*, 400.

(22) (a) Payrastre, C.; Obaya, N.; Madaule, Y.; Wolf, J. G. *Tetrahedron Lett.* **1994**, *35*, 3059. (b) Mazières, M. R.; Romanenko, V. D.; Gudima, A. O.; Payrastre, C.; Sanchez, M.; Wolf, J. G. *Tetrahedron* **1995**, *51*, 1405. (c) Mazières, M. R.; Fialon, M. P.; Payrastre, C.; Wolf, J. G.; Sanchez, M.; Madaule, Y.; Romanenko, V. D.; Chernega, A. N.; Gudima, A. O. *Phosphorus, Sulfur Silicon* **1996**, *109*, 621.

(23) Ulman, A.; Willand, C. S.; Kohler, W.; Robello, D. R.; Williams, D. J.; Handley, L. *J. Am. Chem. Soc.* **1990**, *112*, 7083.

(24) Kanis, D. R.; Marks, T. J.; Ratner, M. A. *Int. J. Quantum Chem.* **1992**, *43*, 61.

**Table 2. Atomic Coordinates and Equivalent Isotropic Displacement Parameters for (ephem)($BF_4$)[a]**

| | *x*/*a* | *y*/*b* | *z*/*c* | $U_{eq}$ |
|---|---|---|---|---|
| C(1) | −0.6943(4) | −0.0774(5) | −0.6179(3) | 0.0394 |
| C(2) | −0.6346(4) | 0.0302(5) | −0.6659(3) | 0.0410 |
| C(3) | −0.6840(4) | 0.1776(5) | −0.6962(3) | 0.0393 |
| C(4) | −0.6281(4) | 0.2756(6) | −0.7513(3) | 0.0472 |
| C(5) | −0.6867(4) | 0.4097(5) | −0.7909(3) | 0.0404 |
| C(6) | −0.8202(4) | −0.0679(5) | −0.5925(2) | 0.0385 |
| C(7) | −0.9144(4) | −0.0154(5) | −0.6458(3) | 0.0418 |
| C(8) | −1.0302(4) | −0.0170(6) | −0.6212(3) | 0.0483 |
| C(9) | −1.0608(4) | −0.0753(6) | −0.5427(3) | 0.0496 |
| C(10) | −1.1919(5) | −0.0813(7) | −0.5176(4) | 0.0683 |
| C(11) | −0.9694(5) | −0.1300(6) | −0.4900(3) | 0.0542 |
| C(12) | −0.8507(4) | −0.1268(5) | −0.5137(3) | 0.0469 |
| C(13) | −0.8165(4) | 0.4385(5) | −0.7742(2) | 0.0364 |
| C(14) | −0.9023(4) | 0.3462(6) | −0.8134(3) | 0.0466 |
| C(15) | −1.0227(4) | 0.3673(6) | −0.7962(3) | 0.0564 |
| C(16) | −1.0571(4) | 0.4832(6) | −0.7387(3) | 0.0526 |
| C(17) | −1.1886(5) | 0.5085(9) | −0.7210(4) | 0.0833 |
| C(18) | −0.9687(5) | 0.5736(6) | −0.6995(3) | 0.0551 |
| C(19) | −0.8482(4) | 0.5536(5) | −0.7159(3) | 0.0482 |
| C(20) | −0.6975(4) | 0.6208(5) | −0.8991(3) | 0.0422 |
| C(21) | −0.6687(4) | 0.8001(6) | −0.8808(3) | 0.0471 |
| C(22) | −0.7711(4) | 0.9058(5) | −0.9158(3) | 0.0419 |
| C(23) | −0.8837(4) | 0.8969(5) | −0.8834(3) | 0.0427 |
| C(24) | −0.9803(4) | 0.9820(5) | −0.9167(3) | 0.0490 |
| C(25) | −0.9651(5) | 1.0815(6) | −0.9840(3) | 0.0595 |
| C(26) | −0.8520(5) | 1.0960(6) | −1.0165(3) | 0.0601 |
| C(27) | −0.7550(4) | 1.0094(6) | −0.9827(3) | 0.0537 |
| C(28) | −0.6806(5) | 0.5753(6) | −0.9910(3) | 0.0563 |
| C(29) | −0.5019(4) | 0.4858(7) | −0.8582(4) | 0.0674 |
| C(30) | −0.5185(4) | −0.2493(6) | −0.6046(3) | 0.0535 |
| C(31) | −0.4868(6) | −0.4067(8) | −0.5616(4) | 0.0825 |
| N(1) | −0.6318(3) | 0.5041(5) | −0.8444(2) | 0.0470 |
| O(1) | −0.6421(3) | −0.2157(4) | −0.5873(2) | 0.0481 |
| O(2) | −0.5577(3) | 0.8418(4) | −0.9166(2) | 0.0622 |
| B(1) | −0.6784(4) | −0.489(1) | −0.2248(4) | 0.0682 |
| F(1) | −0.7804(4) | −0.499(1) | −0.1998(3) | 0.2110 |
| F(2) | −0.6334(9) | −0.6394(9) | −0.2299(6) | 0.2499 |
| F(3) | −0.5904(5) | −0.4309(8) | −0.1779(3) | 0.1750 |
| F(4) | −0.6687(4) | −0.4384(9) | −0.3053(2) | 0.1744 |

[a] Esd's in parentheses refer to the last significant digit. $U_{eq}$ is defined as the arithmetic mean of $U_{ii}$.

**Table 3. Molecular Hyperpolarizability (Vectorial Part of $\beta$) Calculated at Different Laser Frequencies for (ephem)($BF_4$)**

| wavelength ($\mu$m) | hyperpolarizability ($10^{-30}$ cm$^5$ esu$^{-1}$) |
|---|---|
| ∞ | 10.7 |
| 1.907 | 14.5 |
| 1.064 | 34.9 |

to investigate the nature of the atomic orbitals involved in the molecular NLO response.

It has long been recognized that the longest wavelength absorption band of "push−pull" polyene derivatives is responsible for the second-order NLO response, according to the well-known and widely used "two-level model".[25] In this model, the hyperpolarizability ($\beta$) can be described in terms of a ground and first excited-state having charge-transfer character and is related to the energy of the optical transition ($E$), its oscillator strength ($f$), and the difference between ground and excited-state dipole moment ($\Delta\mu$) through the relation

$$\beta \propto f\Delta\mu/E^3$$

The main features associated to the first low-lying optical transitions are shown in Table 4. It must be

(25) Oudar, J. L.; Chemla, J. *J. Chem. Phys.* **1977**, *66*, 2664.

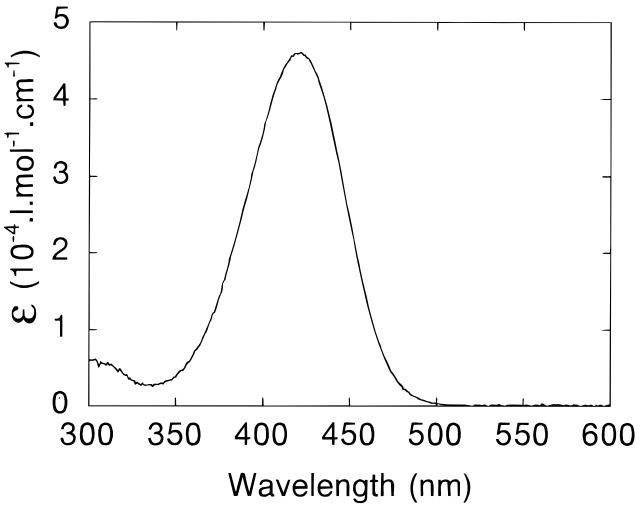


**Figure 2.** Optical spectrum of ephem recorded in $CH_2Cl_2$.

**Table 4. Energies ($\lambda_{max}$ in nm), Oscillator Strengths ($f$), and Dipole Moment Changes between Ground and Excited State ($\Delta\mu$ in D) for the First Excited State of (ephem)($BF_4$)**

| transition | $\lambda_{max}$ | $f$ | $\Delta\mu$ |
|---|---|---|---|
| 1 → 2 | 400 | 1.061 | 8.4 |
| 1 → 3 | 331 | 0.009 | 15.5 |
| 1 → 4 | 290 | 0.002 | 16.7 |
| 1 → 5 | 285 | 0.210 | 11.7 |

pointed out that the agreement between theory and experiment is excellent as shown by comparing Table 4 and Figure 2. The optical properties can readily be described as a single intense band centered at 420 nm. The lowest energy (1 → 2) transition reported in Table 4 is the only one to account for the observed transition, as suggested by a large oscillator strength. The difference in electronic populations between the ground and the first excited states (transition 1 → 2) is shown in Figure 3. Although the expected donor (EtO) and acceptor (C═$N^+$) fragments of (ephem)($BF_4$) are involved in the HOMO and LUMO frontier orbitals, their contribution is not dominant in the intramolecular charge transfer. The nitrogen is responsible for 5% of the overall withdrawing effect in the chromophore (Figure 3 c), while the effect of the ethoxy group is negligible. More surprisingly, one aromatic substituent is found to act as a donor although it bears no strong donor substituent. In summary, the conjugated carbon backbone is mainly responsible for the intramolecular charge transfer and, hence, the NLO response.

**Bulk Susceptibility.** The efficiencies recorded at different laser frequencies are gathered in Table 5. The results recorded at 1.907 $\mu$m clearly show a trend for higher efficiencies as the size of the particles is becoming larger, with an efficiency around 20 times that of urea. This tendency indicates that (ephem)($BF_4$) is phase matchable,[18a] a situation highly desirable for practical use of the material as single crystals. Surprisingly, the efficiencies recorded at 1.064 $\mu$m are not so large, although the hyperpolarizability rises from $14.5 \times 10^{-30}$ cm$^5$ esu$^{-1}$ (at 1.907 $\mu$m) to $34.9 \times 10^{-30}$ cm$^5$ esu$^{-1}$ (at 1.064 $\mu$m). This behavior is usually observed when the second harmonic light is partially absorbed by the chromophore. In the case of (ephem)($BF_4$), absorption cannot be the major reason for a weaker SHG value at

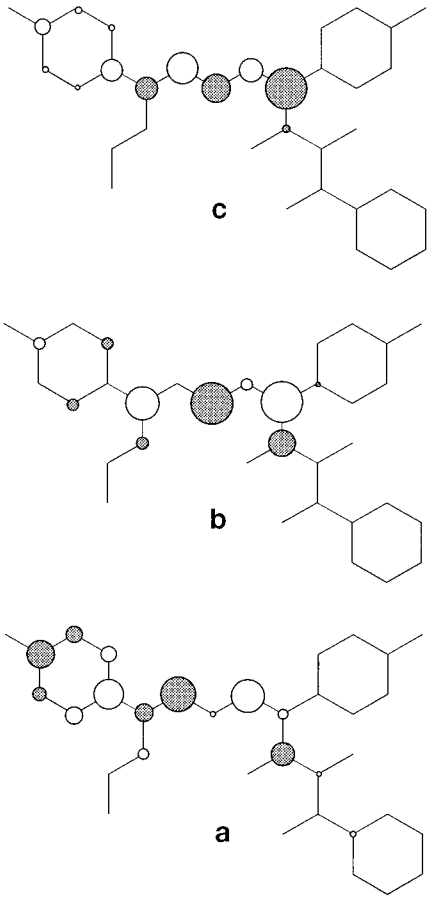


**Figure 3.** Frontier orbitals HOMO (a) and LUMO (b) for (ephem)($BF_4$). (c) represents the difference in electronic populations between the ground and the excited state for the 1 → 2 transition involved in the NLO response.

**Table 5. Powder Efficiencies in Second Harmonic Generation ($I_{2\omega}/I_{\omega}$) versus That of Urea Recorded at Different Laser Frequencies on Calibrated (ephem)($BF_4$)**

| | powder efficiencies | |
|---|---|---|
| grain caliber ($\mu$m) | 1.907 $\mu$m | 1.064 $\mu$m |
| 50−80 | 16.5 | 2.7 |
| 80−125 | 17.5 | 3.1 |
| 125−180 | 21.5 | 2.9 |

1.064 $\mu$m compared to 1.907 $\mu$m. Light scattering is a very influential factor on the amount of second harmonic light that comes throughout the sample. Since scattering is wavelength dependent, values from experiments at different fundamental wavelengths cannot be easily compared. A particularly strong signal loss at 532 nm has been observed on (ephem)($BF_4$).

The relations between microscopic and macroscopic second-order optical nonlinearities have been extensively investigated for any noncentrosymmetric crystal point group by Zyss.[26] The hyperpolarizability tensor (components $\beta_{ijk}$ in the molecular frame) is related to the corresponding crystalline first-order nonlinearity $\chi^2$ (components $d_{IJK}$ in crystalline frame) through the following relation:

$$d_{IJK}(-2\omega;\omega,\omega) = Nf_I^{2\omega}f_J^{\omega}f_k^{\omega}\sum\cos(I,i)\cos(J,j)\cos(K,k)\beta_{ijk}$$

$N$ is the number of chromophores per unit volume, and

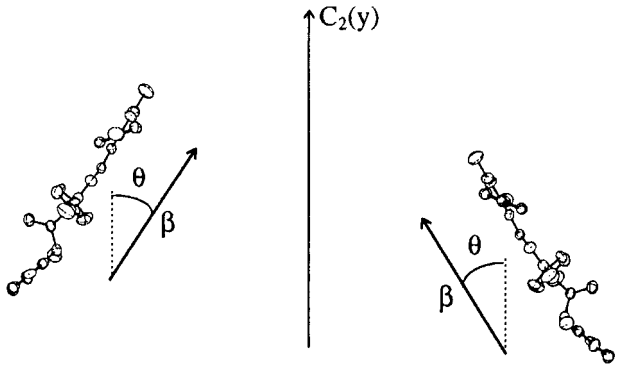


**Figure 4.** CAMERON view of (ephem)($BF_4$) showing the angle ($\theta$ = 39.2°) between $\beta$ and the $C_2$ hellicoidal axis. The $BF_4^-$ anions are omitted.

$f_I^{2\omega}$, $f_J^{\omega}$, and $f_k^{\omega}$ are Lorentz local-field factors. The summation is performed over all molecules in the unit cell, and the cosine product terms represent the rotation from the molecular reference frame into the crystal frame. The molecule presented in our paper crystallizes in space group $P2_1$ (monoclinic point group 2), which has been described in great details elsewhere for the well-known MAP[27] and NPP[28] molecules. Assuming a simplified one-dimensional description of the molecular nonlinear tensor of the molecules, $\beta$ has only one nonvanishing coefficient along the charge-transfer axis $x$ of the molecule (namely $\beta_{xxx}$). This model leads to

$$d_{ZXX} = N\beta_{xxx}\cos\theta\sin^2\theta$$

$$d_{ZZZ} = N\beta_{xxx}\cos^3\theta$$

all other components of the tensor are negligible ($\theta$ is defined as the angle between the main intramolecular charge-transfer axis 0$x$ and the 2-fold axis 0$Z$ of the crystal). The optimization of $d_{ZZZ}$ can be achieved with $\theta$ = 0°, situation which is of no use for birefringence phase matching, and must therefore be avoided. More importantly, the angular factor weighting $\beta_{xxx}$ in the expression of $d_{ZXX}$ is maximized and equal to 0.385 for $\theta$ = 54.74°. Any phase-matching configuration emphasizing this coefficient is to be considered as highly desirable. The orientation of $\beta$ in the crystal cell is shown in Figure 4. In the case of (ephem)($BF_4$) $\theta$ reaches a value of 39.2° and an angular factor of 0.310, which indicates that the orientation of the molecule is not far from being optimized.

## Conclusion

(ephem)($BF_4$) is a new pentamethinium salt easy to obtain as large single crystals with good transparencies in the visible area. The observation that this compound is efficient in SHG with a situation of phase matching opens new perspectives for these derivatives. In the search toward SHG molecular materials, early efforts focused on simply maximizing the strength of the electron donors and acceptors to achieve increased molecular hyperpolarizability. However, Marder et al.

(26) Zyss, J.; Oudar, J. L. *Phys. Rev. A* **1982**, *26*, 2028.
(27) Oudar, J. L.; Zyss, J. *Phys. Rev. A* **1982**, *26*, 2016.
(28) Zyss, J.; Nicoud, J. F.; Coquillay, M. *J. Chem. Phys.* **1984**, *81*, 4160.

have established that the strength of an electron donor and electron acceptor must be optimized for the specific $\pi$-system in order to achieve the maximum hyperpolarizability.[29] Hence, there is a need to "tune" rather than "maximize" the donor and acceptor strength in chromophores such as ephem$^+$. Our study reveals that pentamethinium salts can exhibit larger molecular hyperpolarizabilities than donor−acceptor substituted benzene such as *p*-nitroaniline. The fact that the carbon backbone plays the essential role in the hyperpolarizability suggests that a set of appropriate substitutions on the aromatic ring would optimize $\beta$ and expectingly the efficiency of the materials. We are currently investigating this possibility.

(29) Marder, S. R.; Beratan, D. N.; Cheng, L. T. *Science* **1991**, *252*, 103.

**Supporting Information Available:** Experimental details and tables of atomic coordinates, anisotropic parameters, and bond lengths and angles (10 pages). Ordering information is given on any current masthead page.

CM970734J